Insights into the roles of recently developed coagulants as pretreatment to remove effluent organic matter for membrane fouling mitigation

Viet Ly Quang[a], Long D Nghiem[b], Jinwoo Cho[a], and Jin Hur[a,*]

[a]Department of Environment & Energy, Sejong University, Seoul 143-747, South Korea

[b]Centre for Technology in Water and Wastewater, University of Technology Sydney, Ultimo, NSW 2007, Australia

Revised and Re-submitted to *Journal of Membrane Science*, July, 2018

* Corresponding author:

Tel. +82-2-3408-3826;

Fax +82-2-3408-4320.

E-Mail: jinhur@sejong.ac.kr

Abstract

Membrane fouling by dissolved organic matter (EfOM) in secondary treated effluent is a problematic and inevitable issue during wastewater reclamation using low pressure membrane filtration. This study evaluates the performance of coagulation/flocculation (C/F) using two recently developed coagulants (namely $TiCl_4$ and $ZrCl_4$) in comparison to conventional alum (i.e. $Al_2(SO_4)_3$) as pretreatment to remove EfOM for subsequent ultrafiltration (UF) membrane fouling mitigation. At the optimal dosage, $TiCl_4$-based C/F pretreatment showed the greatest performance in membrane fouling mitigation, followed by $ZrCl_4$ and then alum. The underlying mechanisms were well explained by classical fouling models and the extended Derjaguin-Landau-Verwey-Overbeek (xDLVO) theory, highlighting a dominant role of standard blocking in the fouling potential of the C/F treated EfOM. The interfacial free energy of cohesion and adhesion showed that C/F pretreatment using $TiCl_4$ and $ZrCl_4$ as coagulant can lower the binding affinity between EfOM molecules and between EfOM molecules and membrane surface, ultimately reduce membrane fouling. The results of size exclusion chromatography (SEC) and fluorescence excitation emission matrix- parallel factor analysis (EEM-PARAFAC) also supported the classical fouling mechanisms, providing additional insights into the potential roles of chemical interactions in the preferential removal of certain organic substances by C/F pretreatment and the chemical composition of subsequent membrane foulants. Protein-like components were highly associated with reversible fouling after the C/F, while the reversibility of humic-like substances was enhanced upon C/F pretreatment. After C/F pretreatment, small sized EfOM molecules became the dominant fraction responsible for UF membrane fouling.

Keywords: Wastewater reclamation, enhanced coagulation, membrane fouling, xDLVO theory, EEM-PARAFAC.

1 Introduction

Water reclamation is an important and arguably most sustainable and cost-effective practice to address water shortage in highly populated areas [1]. In this context, ultrafiltration (UF) has emerged as a preferred treatment option due to its capability to remove a broad range of contaminants, including colloids, bacteria, pathogens, and other organic pollutants, as well as low energy consumption compared to high pressure membrane processes (e.g., nanofiltration and reverse osmosis) [2, 3]. However, membrane fouling is a major technical challenge to cost-effective implementation of UF for water reclamation [2]. Fouling of UF membrane is typically governed by the composition of effluent dissolved organic matter (EfOM), which is mostly produced during biological wastewater treatment [4, 5]. EfOM contains various organic materials consisting of polysaccharides, proteins, humic substances (HS), amino sugars, and nucleic acids, which originate primarily from soluble microbial products (SMP) and uncharacterized refractory dissolved organic matter (DOM) [6, 7]. High molecular weight (MW) biopolymers and HS are major contributors to UF membrane fouling [5, 8]. There is also evidence that other organic constituents can be involved in the fouling process. For example, a previous report has shown a connection between neutral and low MW organics and membrane fouling potential [9].

Several treatment options prior to UF filtration have been proposed to address membrane fouling mitigation. In particular, coagulation/flocculation (C/F) is probably the most widely used and effective method to reduce membrane fouling and to enhance the subsequent filtration performance [10-12]. C/F can remove a fraction of DOM as well as particulate matters, thus improving the membrane filterability in subsequent processes [3, 11]. The effectiveness of C/F processes towards the fouling mitigation depends upon the types of coagulants, the C/F

conditions, and the characteristics of the wastewater to be treated [13]. Recently, Ti- and Zr-based coagulants have been introduced and received much attention due to their enhancement in DOM removal [14-16] and membrane fouling alleviation [17] over the conventional coagulant (alum, $Al_2(SO_4)_3$). Their superior performance may be related to many factors including floc growth rate, the size, and the structures, as well as a variety of hydrolyzed species produced and the involved complex interactions (e.g., charge neutralization, adsorption, and sweep coagulation) [13, 15, 18, 19]. For instance, highly charged hydrolysis products of the novel coagulants, such as $(Zr(OH)_2.4H_2O)_4^{8+}$, $Zr_3(OH)_3^{8+}$, $Zr(OH)(OH_2)_7^{3+}$, have been proposed to play a crucial role in enhancing the destabilization of suspension and creating differences in DOM quantity and composition of treated samples from those of the traditional Fe- or Al-based coagulants [15, 16]. Despite the successful applications of the novel coagulants, however, most studies to date have focused on the drinking water sources [15-17, 20]. There are only a few studies available to compare the performance of the novel versus the conventional coagulants on the removal of wastewater [21, 22], in which the removal efficiencies of different coagulants were compared based on the bulk EfOM parameters such as chemical oxygen demand [22], dissolved organic carbon (DOC) [21]. However, it is notable that these bulk parameters provide little information on EfOM composition [7]. To date, there has been no effort in the literature to explore the pretreatment performance of these novel coagulants on the removal of EfOM through the post-treatment of membrane filtration and the subsequent membrane fouling mitigation.

Fluorescence excitation mission matrix coupled with parallel factor analysis (EEM-PARAFAC) is of great merit in obtaining detailed information on the distributions of different fluorophores in DOM due to its capability to decompose bulk DOM into several fluorescent components with specific characteristics and structures [23]. EEM-PARAFAC has recently

become a popular and useful tool to probe the dynamic changes in EfOM for natural and engineering systems [4, 24-26]. However, EEM-PARAFAC is not able to reflect non light-absorbing constituents (e.g., (poly)saccharides) [27]. Size exclusion chromatography (SEC) equipped with organic carbon detector (SEC-OCD) [28] can be a good complementary tool to overcome the limitation. The combined use of SEC-OCD and EEM-PARAFAC has proven its powerful benefit in tracking the fate of different EfOM constituents upon many treatment processes [4, 24, 29]. Yet, there was no study to utilize such advanced DOM analyses for the evaluation of the novel coagulants as the pretreatment for membrane filtration.

The extended Derjaguin, Landau, Verwey and Overbeek (xDLVO) theory can describe the fouling potential of biologically-derived organics on membrane surface via three different interactions including van der Waals (LW), electrostatic (EL) and acid-base interactions [30, 31]. Despite its ability to unravel the underlying mechanisms associated with the interactions between DOM and membrane, only a few studies have adopted the theory to explain the pretreatment effects on membrane fouling such as chlorination [32] or ozonation [33]. It remains unanswered whether this approach can also be practical to the C/F as a pretreatment to membrane filtration. This study aims to (1) to comprehensively compare the performance of three coagulants, including $TiCl_4$, $ZrCl_4$, and $Al_2(SO_4)_3$ (alum), as the pretreatment option to UF for wastewater reclamation, and (2) explore the underlying mechanisms of UF membrane fouling mitigation by the xDLVO theory and advanced DOM analyses.

2 Materials and Methods

2.1 Coagulation/flocculation (C/F) experiments

Biologically treated wastewater was collected after gravity clarification from a municipal wastewater treatment plant in Seoul, South Korea. The collected sample was filtered through 0.45 μm (cellulose acetate, Advantec) and was denoted as EfOM. DOC concentration and UV absorption coefficient at 280 nm (UV_{280}) of this wastewater sample were 5.7±0.3 mgC/L and 0.12±0.03 1/cm, respectively. This biologically treated wastewater has a pH of 6.8.

Aluminum sulfate ($Al_2(SO_4)_3 \cdot 18\ H_2O$), zirconium chloride ($ZrCl_4$), and titanium chloride ($TiCl_4$) were purchased from Sigma Aldrich and were used as coagulants. Stock solutions were prepared in 2000 mg-metal/L by adding the corresponding amounts of the metal coagulants into Milli-Q® water (Rephile, US). The C/F experiments were conducted using a jar test apparatus (C-JT, Chang Shin Science). Each C/F experiment consisted of 2 min rapid mixing at 200 rpm, followed by flocculation for 20 min at 30 rpm. After 30 min settling, the supernatant was carefully taken at 3 cm below the solution surface for the measurements of zeta potential values using a Zetasizer (model 380 ZLS, PSS NICOMP). All C/F experiments were conducted in duplicate. The supernatant was adjusted to pH 3 prior to fluorescence measurements to prevent potential quenching effect of multi-valent cations on the fluorescence spectra [34]. C/F treated samples were filtered through 0.45 μm membrane filter (Advantec, Japan) to remove particulate matter, re-adjusted to pH 7.0, and used for subsequent UF experiments.

2.2 UF membrane filtration and the estimation of membrane fouling potential

A flat-sheet polyethersulfone (PES) membrane with a molecular weight cutoff (MWCO) of 30 kDa was purchased from Pall Corp. (USA). The membrane surface contact angle was

51.4±2.4°. The zeta potential of this membrane was previously reported to be -14 mV at pH 7.0 in 10 mM KCl solution [35]. The membrane was submerged in distilled deionized water (DDW) for 48 hours before use.

UF experiment was conducted using a 400 mL dead-end stirred cell (Amicon 8400, Millipore Corp., USA) with an effective filtration area of 41.8 cm^2. A pressurized nitrogen cylinder was connected to the UF unit to maintain a constant pressure of 0.03 MPa. Water permeability of the clean membrane was 99.2±1.0 $L/m^2/h$. Detailed descriptions of the UF operation and the extraction method for foulants are available elsewhere [36, 37]. Briefly, the UF filtration was operated in three cycles using 330 mL-feed solution at a neutral condition. Each cycle was terminated when 300 mL of permeate solution was obtained. DDW (50 mL) was used to backwash the reversible foulant from the membrane surface. The membrane was reversed, and DDW (200 mL) was filtered to test irreversibility after hydraulic backwashing. Irreversible foulants after the three cycles of the filtration was removed by submerging the membrane into 0.1 N NaOH solution for 30 min in a shaker at 150 rpm. The irreversible foulant solution was re-adjusted to pH 7.0. All UF experiments were conducted in duplicate.

The unified membrane fouling indices (UMFI) were calculated based on the following equations [38]:

$$UMFI_{Total} = (J_o/J - 1)/V \quad (1)$$

$$UMFI_{IR} = (J_o/J - 1)/V \quad (2)$$

$$UMFI_{Re} = UMFI_{Total} - UMFI_{IR} \quad (3)$$

The subscript ‘Total’, ‘IR’ and ‘Re’ denote total, irreversible, and reversible fouling, respectively. Since the normalized flux (i.e., J_o/J) is not linearly correlated with specific permeate volume (V), the membrane fouling indices were determined based on the 2-point method [39].

158 $UMFI_{Total}$ values were acquired using the slopes of the lines connecting the first flux data point
159 from the first cycle for EfOM and the last flux data point from the third cycle. $UMFI_{IR}$ values
160 were obtained based on the initial flux data point of the first cycle and the last flux data point for
161 DDW backwashing before chemical cleaning [38, 39]. The schematic diagram is in Fig. S1.
162
163 *2.3 Analytical methods*
164 *2.3.1 DOC measurements and UV-visible (UV-Vis) spectroscopy*
165 A TOC analyzer (Shimadzu TOC-L, Japan) was employed to obtain DOC concentrations.
166 UV absorption coefficient at 280 nm was determined using a Shimadzu spectrophotometer
167 (model UV-1800) with a 1-cm quartz cuvette.
168
169 *2.3.2 Fluorescence EEM measurements and PARAFAC modeling*
170 Fluorescence EEM spectra were obtained in a luminescence spectrometer (Hitachi F-
171 7000 FL, Japan) by scanning EfOM samples at the emission wavelength (Em) from 280 to 550
172 nm at 1 nm-resolution and stepping through the excitation wavelength (Ex) from 220 to 500 nm
173 at 5 nm intervals. Excitation and emission slits were both adjusted at 10 nm. The scan speed was
174 set at 12000 nm/min. To limit second order Raleigh scattering, a 290 nm cut off filter was used
175 for all measurements. The fluorescence response to DDW was considered as a blank
176 (background) EEM of each sample. The inner filter correction was neglected by a sample
177 dilution method [40]. Fluorescence intensity was normalized using Raman unit equivalents (RU)
178 [41]. PARAFAC modeling was conducted using MATLAB 7.1 (MathWorks, Natick, MA, USA)
179 with the DOMFluor Toolbox [42]. The identified fluorescent components were validated by split
180 half and residual analysis. Maximum fluorescence intensities (F_{max}) of the identified fluorescent

DOM (FDOM) components were used to indicate their relative concentrations. The portion of each FDOM component in different compartments (i.e. permeate, concentrate, reversible and irreversible solutions) was determined for the mass balance calculation by multiplying their F_{max} values with the corresponding solution as described in the recent literature [4, 25, 36, 37].

2.3.3. Size exclusion chromatography

A size exclusion chromatography (SEC) system (Model 7, DOC-Labor, Germany), equipped with both OCD and ultraviolet detector (UVD), was employed to compare the MW distributions of EfOM samples before and after UF filtration [28]. Each sample (1000 µL) was injected at flow rate of 1.1 mL/min for a retention time of 130 min. Five different size fractions were quantified from the SEC chromatograms, which included biopolymer (BP) (>20k Da), humic substances (HS) (1k Da), building blocks (BB) (500 Da), low molecular weight organics (LMW organics) (350 Da) based on the respective retention times and the shapes [28]. The concentrations of the individual size fractions were determined by a software installed in the system (Chrom CALC, DOC-Labor, Germany). A separate SEC system with a fluorescence detector was also utilized for this study to complement the molecular size information on different FDOM components (Supplemental Information, SI).

2.3.4 Interaction energy analysis

According to the xDLVO theory, interfacial energy between membrane and the foulants is related to surface tension, which can be determined by the contact angle between a reference liquid and the solid surface. Three reference liquids [43] were used for this study. They include one apolar liquid (diiodomethane; CAS: 75-11-6, Sigma-Aldrich, USA) and two polar (DDW

and glycerin; CAS: 56-81-5, Sigma-Aldrich, USA) liquids. The reported surface tension properties of the liquids are summarized in Table S1. Contact angle was measured via the sessile drop method using SmartDrop (Femtofab, South Korea). Before the measurement, the membrane was first conditioned and dried, following a protocol previously reported in the literature [33]. To assess the effects of the C/F pretreatment, 3 L of the untreated and C/F-treated EfOM samples was filtered through the UF membrane. A piece of the membrane was cut and attached to the stainless steel plate with the fouling layer facing upward. The reference liquid (5 µL) was then deposited onto fouled membrane surface using a micro-syringe. Contact angle on both sides of the droplet recorded. All contact angle measurements were conducted in triplicate.

3 Results and Discussion

3.1 Dynamic variations of DOC upon the C/F processes using different coagulants

EfOM removal by the three coagulants was compared in terms of DOC (Fig. 1). EfOM removal steadily increased as the coagulant dosage increased for all three coagulants. At coagulation dosage above 20 mg/L, the rate of EfOM removal increase was significant for $ZrCl_4$ and $TiCl_4$. On the other hand, the increase in EfOM removal by alum was insignificant when alum dosage increased beyond 20 mg/L. Overall, EfOM removal by either $ZrCl_4$ or $TiCl_4$ was higher than that by alum, indicating their superior removal capability for EfOM over the conventional coagulant (i.e., alum) (Fig. 1). $TiCl_4$ was the most effective among the three coagulants in this study, followed by $ZrCl_4$ and alum. EfOM removal efficiency observed in this study was lower than the removal of aquatic humic substances using the same coagulants (e.g. up to 90% by $ZrCl_4$ [44] or $TiCl_4$ [20]) at a similar coagulant dosage. Results in this study suggest

that EfOM is more resistant to the C/F treatment than aquatic humic substances. This difference may be attributed to the unique characteristics of EfOM in comparison to humic substances [45, 46].

Surface charge of flocs particles measured by zeta potential can provide further insight to the removal mechanisms of DOM by C/F [10]. Zeta potential of EfOM samples after C/F exhibited a sharp increase from -10.8 to +6.5 mV due to alum addition up to 25 mg/L. Beyond the alum dosage, the increase in zeta potential of the flocs was more gradual (e.g., +7.4 mV at 80 mg/L of alum) (Fig. 1b). In contrast, when $TiCl_4$ and $ZrCl_4$ were used as coagulants, zeta potential of the resulted flocs increased steadily as the coagulant dosage increased (Fig. 1b). Similar observation has been reported for surface water [15] and humic substances [17, 20]. From Fig. 1b, isoelectronic point (IEP) could be identified when the coagulant dosage reached 15, 80, and 80 mg/L for alum, $TiCl_4$, and $ZrCl_4$, respectively. These values were close to the dosages corresponding to the respective maximum or near-maximum removal rates over the tested dosages. This observation implies that charge neutralization plays a critical role in the C/F processes for EfOM removal. The increase in DOC removal as the alum dosage increased beyond 20 mg/L (Fig. 1) suggests that charge neutralization might not be a sole mechanism to operate in the EfOM removal. It is possible that, at high alum dosage, adsorption and enmeshment/sweep coagulation could overshadow the destabilization of EfOM molecules maintained by repulsive charge interaction [10], in which the precipitation of metal hydroxides might occur due to the dominant presence of soluble metal species [13]. The enhanced removal rates of EfOM by $TiCl_4$ and $ZrCl_4$ versus alum were consistent with the previous studies based on surface water DOM, which was explained by the greater charge neutralization capacity of the highly charged cationic hydrolyzing species of the two novel coagulants versus alum [15, 16].

3.2 *Removal behaviors of different EfOM constituents upon the C/F processes*

3.2.1 *Different fluorescent components*

Three different FDOM components were identified by PARAFAC (Fig. 2). Component 1 (C1) exhibited two maxima at 230/340 nm (Ex/Em) and 270/340 nm (Ex/Em). It is denoted as a protein-like component, which relates to microbial activities [4, 24]. Component 2 (C2) displayed two peaks at 240/440 nm (Ex/Em) and 340/440 nm (Ex/Em). Similar fluorescence peaks were reported for humic substances with terrestrial sources [47, 48] as well as microbial-derived humic substances [4, 6]. The peaks of component 3 (C3) appeared at Ex/Em of 240/360 nm and 270/360 nm, which resembled a traditional protein-like fluorophore with microbial origins [25, 49].

The general removal behavior (i.e., increased removal with a higher dose) of all three FDOM components was similar to that measured by DOC (i.e., bulk parameter) irrespective of the coagulant types. However, the relative removal extent at a given dosage was different by the FDOM components, suggesting an unique set of characteristics of individual FDOM components in response to the C/F process. The C1 showed consistently higher removal rates than the C3 regardless of the coagulants and dosages (Fig. 3). For example, the removal rates of C1 and C3 were 39.3 and 4.8%, respectively, at 20 mg/L for alum. This observation is interesting since C1 and C3 components are both protein-like fluorophores presumably microbial origin. Fluorescence-detected SEC chromatograms revealed the two protein-like components might be discriminated by different molecular sizes as shown in Fig. S2. However, molecular size alone cannot fully explain the different removal rates between C1 and C3 because the humic-like C2 showed a higher removal rate than C3 despite its smaller molecular size (Fig. S2). The literature

has suggested that humic-like components are more hydrophobic than protein-like components [7, 50]. In addition, the hydrophobic DOM fraction is more readily removed by C/F processes than the hydrophilic one [13, 51]. Yuan et al. [52] reported that the DOM samples with higher O/C ratios were removed to a greater extent by C/F processes. Overall, results from our study imply that both molecular sizes and chemical composition of DOM (or EfOM) can govern organic removal by C/F.

Similar to the bulk DOM removal, the FDOM components (particularly, C2 and C3) generally showed the higher removal rates upon the addition of $TiCl_4$ and $ZrCl_4$ versus alum (Fig. 3), which agreed with a previous study using aquatic DOM [15]. However, the relative differences depended on the types of the coagulants and the FDOM components, which may be ascribed to the unique characteristics of the two novel coagulants. For example, previous reports suggested that $TiCl_4$ resulted in a faster floc growth rate and larger floc sizes than alum, while $ZrCl_4$ was the superior to remove relatively low MW organics [15, 20]. Further study is warranted to fully explain the C/F-dependent removal tendencies towards the different FDOM components.

3.2.2. Different size fractions

The removal rates of different EfOM size fractions were compared at the fixed dosage of each coagulant (20 mg/L for alum and 40 mg/L for $TiCl_4$ and $ZrCl_4$). The dosages were chosen based on the trends showing no significant improvement in EfOM removal with the further addition of the coagulants. For example, the dosages doubled from 40 to 80 mg/L for $ZrCl_4$ and/or $TiCl_4$ resulted in only 15% additional removal (Fig. 1). These dosages also prevent excessive sludge production.

Comparison of the DOC-detected versus UV-detected SEC chromatograms revealed that the largest size fraction (i.e., BP) might be mostly dominated by polysaccharides due to its relatively low UV response versus the high DOC, while LMW organics were enriched with conjugated structures (i.e., high UV signals) (Fig. S3) [4, 53]. The removal of different DOC fraction was in the decreasing order of BP > HS > BB > LMW organics for all three coagulants, showing the preferential removal tendency for large molecular weight organics (Fig. 3d). These results are in a good agreement with literature [3, 54]. Henderson et al [55] reported that the removal behavior of HMW molecules is likely governed by charge neutralization, adsorption, and enmeshment/sweep coagulation, while cross-linking and floc agglomeration with metal hydrolysis products are essential for the removal of LMW molecules. At the dosages chosen, $TiCl_4$ presented the highest removal rates for all four size fractions with the superior capability over other two coagulants. The most pronounced changes were found for the intermediate size fraction (i.e., BB), in which the percent removal was 32.5% for $TiCl_4$ in comparison to 12.5% for alum and 8.4% for $ZrCl_4$ (Fig. 3d).

3.2.3. Flux decline of UF and reversibility of EfOM upon different coagulants

The EfOM samples treated at the designated dosages were used to assess the influence of the C/F on membrane fouling of UF processes. Before the pretreatment, a severe flux decline was observed with the final normalized flux (J/J_o) value of 0.56 at the end, while the C/F treatment led to an obvious improvement in the flux decline (Fig. 4). The mitigation of the membrane fouling was greater in the order of $TiCl_4$ > $ZrCl_4$ > alum with the normalized flux (J/J_o) corresponding to 0.81, 0.68, and 0.65, respectively, after three cycles. The primary reason for the dissimilar effects on the fouling mitigation may lie in the greater removal tendency

318 towards the HMW molecules (i.e., BP and HS fractions), which serve as the main foulants, of the
319 two novel coagulants versus alum (Fig. 3). Close association between membrane fouling
320 potential and HMW organics has been reported in the literature [8, 56]. Results from our study
321 are also consistent with a recent study by Su et al [17], who demonstrated an improved
322 membrane filtration performance for HS by using the novel coagulant, $ZrOCl_2$, versus $Al_2(SO_4)_3$
323 for the C/F prior to membrane filtration.

324 The UMFI values of the untreated EfOM indicated that reversible fouling might contribute
325 more to the total membrane fouling potential than irreversible fouling (i.e., 2.35×10^{-3} m^2/L for
326 $UMFI_{Re}$ versus 1.35×10^{-3} m^2/L for $UMFI_{IR}$) (Fig. 4). Compared to alum, $TiCl_4$ showed a better
327 performance in membrane fouling mitigation with respect to both reversible and irreversible
328 fouling as shown by the much lowered UMFI values (Fig. 4). In contrast, the mitigation effect of
329 $ZrCl_4$ was not so much pronounced as that of alum, particularly for reversible fouling (Fig. 4).

330 Four classic filtration models have been widely employed to evaluate the efficiency of
331 pretreatment to control membrane fouling (Figs. S4, S5 and Table S2) [36, 57]. Without
332 pretreatment, cake filtration and standard blocking seem to be the main mechanisms more
333 responsible for flux declines compared to the intermediate and the complete blocking
334 mechanisms, as demonstrated by the R^2 values of the linear regression for cake/gel layer,
335 standard blocking, intermediate blocking, and complete blocking being 0.952, 0.994, 0.821, and
336 0.832, respectively (Table 1). It has been established that cake/gel layer can be formed by large
337 sized DOM molecules, which are hydraulically reversible [36]. On the other hand, LMW DOM
338 molecules are associated with standard blocking, contributing to irreversible fouling potential
339 [36]. After the C/F processes, the treated EfOM showed the decreases of the R^2 values for all the
340 proposed fouling models except for the standard blocking model (Table 1). This suggests that the

membrane fouling by large sized EfOM molecules was alleviated by the pretreatment, while LMW molecules might be still a dominant fraction causing the membrane fouling of the treated samples. For example, the R^2 values of the cake/gel layer model for the untreated and the treated samples were 0.952 (untreated), 0.792 (alum), 0.752 ($TiCl_4$) and 0.878 ($ZrCl_4$), respectively, while those of the standard model were all above 0.990 (Table 1).

3.3 Understanding of UF membrane fouling from interaction free energy point of view

The measured surface tension parameters and interaction free energies are shown in Table 2. In the current work, the free energy of electrostatic double layer, ΔG^{EL}, was not taken into account since it was previously reported to be very low in biological systems [30]. The virgin PES membrane exhibited a high electron donor component value (δ^-; 22.5 mJ/m^2) and a low electron acceptor component value (δ^+; 0.5 mJ/m^2), signifying a high electron donor monopolarity with apolar feature, which is typically found in polymeric membranes [25, 30]. Like the virgin PES membrane, the membranes treated with the original and the C/F-treated EfOM exhibited relatively high values for electron donor components, which were comparable to those previously reported based on wastewater DOM [33].

The interfacial free energy between the same solid surfaces, which are immersed and remain in contact with an aqueous phase (i.e., water), denoted as cohesion free energy (ΔG_{iLi}) [43]. The more negative or positive values are, the greater extent of hydrophobic or hydrophilic potential can be presumed for the measured materials. Thus, it provides a quantitative insights into the affinity between two similar solid surfaces [30, 31, 43]. In this study, the virgin PES membrane showed a hydrophobic nature with a negative value of cohesion free energy (i.e., -16.20 mJ/m^2). Similarly, a negative value was shown for the untreated EfOM, implying its

thermodynamically instable property to form a hydrophobic matrix [30]. The C/F pretreatment appears to weaken the hydrophobic nature of EfOM components, as shown by the increased values (or less negative values) of the C/F treated versus the untreated EfOM. Among the C/F-treated samples, $TiCl_4$-treated EfOM showed the highest cohesion free energy (ΔG_{iLi}) with a positive value of 3.23 mJ/m^2, indicating that $TiCl_4$-treated EfOM has the lowest binding affinity, followed by $ZrCl_4$- and alum-treated EfOM.

The adhesion free energy (ΔG_{iLm}) reported here represents the affinity potential between EfOM samples and the virgin membrane. Huang et al. [31] suggested that the behavior of organic foulants regarding attachment and deposition of organic foulants on membrane surface can be determined quantitatively by interfacial energy of adhesion. In this study, all the measured EfOM samples, either treated or untreated, exhibited the negative values in the interfacial free energy of adhesion. The lowest value was found for the membrane founded by untreated EfOM (-28.10 mJ/m^2), suggesting that the original EfOM before pretreatment can be strongly attractive to the PES membrane. Once EfOM is treated by the C/F processes, the affinity between the organics and membrane surface was lowered, following the relative order of the novel coagulants > alum. The ΔG_{iLm} values were -8.64 and -6.81 mJ/m^2 for $ZrCl_4$ and $TiCl_4$, respectively, and -15.1 for alum (Table 2).

Regarding the differences between the untreated and the C/F treated EfOM samples, it is noteworthy that the organic matrices, simultaneously containing proteins, polysaccharides, and HS, tend to generate more compact aggregates, exerting a greater membrane fouling potential compared to those consisting of the individual organic components [30, 58-60]. The removal of certain organic constituents by the C/F pretreatment may lead to the lower extent of the intermolecular interactions among different organic molecules as shown by the changes in the

cohesion free energy (Table 2). The phenomenon can make cake/gel layers loosely formed on membrane surface [31, 33]. Taken together, the higher values of the interfacial free energy (i.e., ΔG_{iLi}^{TOT} or ΔG_{iLm}^{TOT}) for the EfOM samples treated by $TiCl_4$ or $ZrCl_4$ versus alum (Table 2) support the outperformance of the novel coagulants over alum as the C/F pretreatment option for membrane fouling mitigation from interaction free energy point of view.

3.4 The fate of different EfOM constituents in reversible/irreversible fouling

3.4.1 Removal rates of FDOM components by C/F-UF process

The removal rates of the individual FDOM components were determined based on the mass balance between the feed and the permeate solutions. The UF process removed C1, C2, and C3 from untreated EfOM at the rate of 55.3±2.3, 16.7±5.9, and 30.1±4.4%, respectively (Fig. 5). The relative order of the removal rates (i.e., C1 > C3 > C2) implies a dominant effect of size exclusion on the removal performance, which is supported by the fluorescence-detected SEC chromatograms which showed more distribution of the SEC signals into HMW (or shorter retention times) in the order of C1 > C3 > C2 (Fig. S2). Size exclusion effect has been suggested in many literature as a dominant mechanism to explain UF processes [5, 9, 24]. Irrespective of the coagulant types (Fig. 5), the C/F pretreatment examined here apparently enhanced the overall removal efficiencies for all the FDOM components in UF process. The greatest enhancement was found for C2 as shown by the largest differences in the removal rates between with and without the C/F pretreatment (Fig. 5).

3.4.2 Relative contributions of FDOM components to reversible/irreversible membrane fouling

A mass balance approach was applied for the individual FDOM components to estimate the relative contributions to reversible and irreversible fouling. The relative contribution of FDOM components in the untreated EfOM to reversible over irreversible fouling was greater for HMW components (i.e., C1 > C3 > C2) (Fig 5). The relative order of different FDOM components with respect to the ratios of reversible to irreversible fouling potential) was kept the same after the pretreatment. Such dissimilar fouling behaviors among the individual FDOM components can be explained by the differences in the molecular sizes and hydrophobicity. For example, smaller sized molecules tend to penetrate deeply and irreversibly adsorb on membrane pores, while humic-like substances may have a strong affinity to bind the hydrophobic PES membrane through hydrophobic interactions [36, 61].

For the two protein-like components, the C/F pretreatment did not result in any significant difference in the relative reversible fouling potential (i.e., Re/(IR+Re)) (ANOVA, $p>0.05$). In contrast, the reversibility was improved for the humic-like C2 by the C/F as indicated by the higher Re/(IR+Re) ratios (Fig. 5). The increased reversible fouling potential could be associated with the interactions between HS and residual multivalent cations upon the C/F. A previous study demonstrated that the addition of multivalent cations (e.g., Ca^{2+} and Al^{3+}) could induce the aggregation of HS, thus increasing their apparent molecular sizes [62, 63]. This phenomenon may shift the fouling mechanism responsible for the C2 component (or HS) partially from inner pore adsorption and clogging (irreversible) into cake/gel layer formation (reversible) [64].

3.4.3 Distributions of different size fractions in membrane fouling solutions

For untreated EfOM, BP was the most dominant fraction present in the reversible solution (65.7%), followed by LMW organics (22.8%) (Fig. 6). The HS and BB fractions were present in only minor portions in the reversible solution (4.2%). The major contribution of BP to reversible fouling can be attributed to the size exclusion of membrane filtration, which leads to the preferential retaining for HMW organics in a form of easily detachable cake/gel layer [2, 64]. The cake/gel layer may further act as a secondary barrier to hold LMW organics [65]. The minor presence of HS and BB fractions in the reversible foulants was consistent with the previous reports [4, 9].

Both HS and LMW organics are major contributors to the irreversible fouling with their relative presence of 41.3 and 42.4%, respectively (Fig. 6). The high association of HS with irreversible fouling is well documented [66]. The contribution of LMW organics to irreversible fouling can be explained by 1) hydrophobic interactions between the PES membrane and the size fraction with enriched aromatic structures (as indicated by their high UV responses in the SEC chromatograms), and 2) the propensity of small sized molecules to penetrate deeply into the membrane matrix, which renders the resistance to hydraulic backwashing [64, 67].

C/F pretreatment using $TiCl_4$ or $ZrCl_4$ coagulant altered the relative contributions of different EfOM size fractions to reversible or irreversible fouling potential (Fig. 6). After C/F treatment, the relative contribution of BP to reversible fouling was declined from 65.7% to ~25%. Such a notable change did not occur for the sample treated by alum-based C/F. The minor presence of both HS and BB in the reversible solution was commonly observed irrespective of the C/F pretreatment (Fig. 6). Meanwhile, LMW organics became more dominant in the reversible fouling solutions after the novel coagulants-pretreatment. For example, the relative

453 contributions were 58.7% and 55.7% after the C/F using $ZrCl_4$ and $TiCl_4$, respectively, which
454 contrasts with 22.8% for the untreated EfOM (Fig. 6). The interactions between LMW organics
455 and residual metal cations appear to modify the LMW organics into relatively larger sized
456 molecules as shown in the emerging peaks of the C/F treated samples (Fig. S3). It is speculated
457 that such compactly formed molecules could be easily trapped by the reversible cake/gel layer
458 acting as a secondary filter [65].

459 For irreversible fouling, the relative contribution of HS was noticeably reduced after
460 pretreatment, while the opposite trend was observed for LMW organics. For example, the
461 relative contributions of LMW organics were 42.4%, 64.1%, 68.2%, and 72.5% for untreated
462 EfOM, and the treated EfOM by alum, $TiCl_4$, and $ZrCl_4$, respectively. The enhanced contribution
463 of LMW organics to irreversible fouling after pretreatment may be attributed to the charge
464 screening effects lowering the repulsive charge interactions with membrane surface [68], which
465 result from increased ionic strength by the presence of residual metal cations (Fig. 1). The
466 increased relative contribution of LMW organics to both reversible and irreversible fouling
467 potentially was consistent with the changes in the fitness of the flux to cake/gel layer model and
468 standard blocking after pretreatment (Table 1).

469

470 **4 Conclusions**

471 Performance of the hybrid C/F-UF process in terms of EfOM removal was
472 systematically evaluated for two recently developed coagulants ($TiCl_4$ and $ZrCl_4$) and a
473 conventional coagulant (alum) using state of the art DOM characterization techniques. SEC-
474 OCD signified the importance of molecular size in the performance of C/F processes, as revealed
475 by the higher removal rates of HMW BP and HS compared to BB and LMW organics. However,

EEM-PARAFAC results revealed the secondary roles of chemical interactions in the C/F performance as C2 (humic-like) component was removed to a greater extent than the protein-like C3 despite its smaller molecular size. The C/F pretreatment enhanced the reversibility of the humic-like C2. The two novel coagulants, particularly $TiCl_4$, outcompeted with alum in the performance of the post UF treatment, exhibiting better membrane fouling mitigation. The relative contribution of LMW organics to reversible membrane fouling was enhanced after the C/F pretreatment using the novel coagulants compared to alum. xDLVO theory, which was utilized for fouling mitigation by C/F pretreatment for the first time in this study, also revealed to be useful for supporting and understanding the mechanisms behind the roles of C/F pretreatment in the post UF treatment. The results from xDLVO analysis suggest that C/F could increase the interfacial free energy of cohesion between EfOM molecular matrices to form relatively less dense aggregates, which subsequently alleviated membrane fouling potential (i.e. reducing the adhesion free energy).

Acknowledgements

This work was supported by a National Research Foundation of Korea (NRF) grant funded by the Korean government (MSIP) (No. 2017R1A4A1015393).

References

[1] J. Burgess, M. Meeker, J. Minton, M. O'Donohue, International research agency perspectives on potable water reuse, Environmental Science: Water Research & Technology, 1 (2015) 563-580.
[2] W. Guo, H.-H. Ngo, J. Li, A mini-review on membrane fouling, Bioresour. Technol., 122 (2012) 27-34.

[3] J. Haberkamp, A.S. Ruhl, M. Ernst, M. Jekel, Impact of coagulation and adsorption on DOC fractions of secondary effluent and resulting fouling behaviour in ultrafiltration, Water Res., 41 (2007) 3794-3802.
[4] Q.V. Ly, L.D. Nghiem, M. Sibag, T. Maqbool, J. Hur, Effects of COD/N ratio on soluble microbial products in effluent from sequencing batch reactors and subsequent membrane fouling, Water Res., 134 (2018) 13-21.
[5] E. Filloux, H. Gallard, J.-P. Croue, Identification of effluent organic matter fractions responsible for low-pressure membrane fouling, Water Res., 46 (2012) 5531-5540.
[6] H. Yu, F. Qu, L. Sun, H. Liang, Z. Han, H. Chang, S. Shao, G. Li, Relationship between soluble microbial products (SMP) and effluent organic matter (EfOM): Characterized by fluorescence excitation emission matrix coupled with parallel factor analysis, Chemosphere, 121 (2015) 101-109.
[7] I. Michael-Kordatou, C. Michael, X. Duan, X. He, D.D. Dionysiou, M.A. Mills, D. Fatta-Kassinos, Dissolved effluent organic matter: Characteristics and potential implications in wastewater treatment and reuse applications, Water Res., 77 (2015) 213-248.
[8] J.-y. Tian, M. Ernst, F. Cui, M. Jekel, Correlations of relevant membrane foulants with UF membrane fouling in different waters, Water Res., 47 (2013) 1218-1228.
[9] R.K. Henderson, N. Subhi, A. Antony, S.J. Khan, K.R. Murphy, G.L. Leslie, V. Chen, R.M. Stuetz, P. Le-Clech, Evaluation of effluent organic matter fouling in ultrafiltration treatment using advanced organic characterisation techniques, J. Membr. Sci., 382 (2011) 50-59.
[10] L. Chekli, E. Corjon, S.A.A. Tabatabai, G. Naidu, B. Tamburic, S.H. Park, H.K. Shon, Performance of titanium salts compared to conventional FeCl3 for the removal of algal organic matter (AOM) in synthetic seawater: Coagulation performance, organic fraction removal and floc characteristics, J. Environ. Manage., 201 (2017) 28-36.
[11] L. Wang, P. Zhang, Y. Li, Pretreatments to control low-pressure membrane fouling: a review on the coagulant/adsorbent applied and contact modes with the feed, Desalination and Water Treatment, 102 (2018) 16-37.
[12] H. Huang, K. Schwab, J.G. Jacangelo, Pretreatment for Low Pressure Membranes in Water Treatment: A Review, Environ. Sci. Technol., 43 (2009) 3011-3019.
[13] A. Matilainen, M. Vepsäläinen, M. Sillanpää, Natural organic matter removal by coagulation during drinking water treatment: A review, Adv. Colloid Interface Sci., 159 (2010) 189-197.
[14] T. Priya, V.L. Mohanta, B.K. Mishra, Performance evaluation of zirconium oxychloride for reduction of hydrophobic fractions of natural organic matter, Sep. Purif. Technol., 174 (2017) 104-108.
[15] S. Hussain, J. van Leeuwen, C.W.K. Chow, R. Aryal, S. Beecham, J. Duan, M. Drikas, Comparison of the coagulation performance of tetravalent titanium and zirconium salts with alum, Chem. Eng. J., 254 (2014) 635-646.
[16] P. Jarvis, E. Sharp, M. Pidou, R. Molinder, S.A. Parsons, B. Jefferson, Comparison of coagulation performance and floc properties using a novel zirconium coagulant against traditional ferric and alum coagulants, Water Res., 46 (2012) 4179-4187.
[17] Z. Su, X. Li, Y. Yang, Y. Fan, Probing the application of a zirconium coagulant in a coagulation-ultrafiltration process: observations on organics removal and membrane fouling, RSC Advances, 7 (2017) 42329-42338.

[18] Y.X. Zhao, B.Y. Gao, H.K. Shon, J.H. Kim, Q.Y. Yue, Effect of shear force, solution pH and breakage period on characteristics of flocs formed by Titanium tetrachloride (TiCl4) and Polyaluminum chloride (PACl) with surface water treatment, J. Hazard. Mater., 187 (2011) 495-501.
[19] Y.X. Zhao, B.Y. Gao, G.Z. Zhang, S. Phuntsho, Y. Wang, Q.Y. Yue, Q. Li, H.K. Shon, Comparative study of floc characteristics with titanium tetrachloride against conventional coagulants: Effect of coagulant dose, solution pH, shear force and break-up period, Chem. Eng. J., 233 (2013) 70-79.
[20] Y.X. Zhao, B.Y. Gao, H.K. Shon, B.C. Cao, J.H. Kim, Coagulation characteristics of titanium (Ti) salt coagulant compared with aluminum (Al) and iron (Fe) salts, J. Hazard. Mater., 185 (2011) 1536-1542.
[21] Y. Okour, H.K. Shon, I. El Saliby, Characterisation of titanium tetrachloride and titanium sulfate flocculation in wastewater treatment, Water Sci. Technol., 59 (2009) 2463-2473.
[22] H.A. Aziz, M.H.A. Razak, M.Z.A. Rahim, W.I.S.W. Kamar, S.S. Abu Amr, S. Hussain, J. Van Leeuwen, Evaluation and comparison the performance of titanium and zirconium(IV) tetrachloride in textile wastewater treatment, Data in Brief, 18 (2018) 920-927.
[23] S.K.L. Ishii, T.H. Boyer, Behavior of Reoccurring PARAFAC Components in Fluorescent Dissolved Organic Matter in Natural and Engineered Systems: A Critical Review, Environ. Sci. Technol., 46 (2012) 2006-2017.
[24] Q.V. Ly, J. Hur, Further insight into the roles of the chemical composition of dissolved organic matter (DOM) on ultrafiltration membranes as revealed by multiple advanced DOM characterization tools, Chemosphere, (2018).
[25] H. Yu, F. Qu, H. Liang, Z.-s. Han, J. Ma, S. Shao, H. Chang, G. Li, Understanding ultrafiltration membrane fouling by extracellular organic matter of Microcystis aeruginosa using fluorescence excitation–emission matrix coupled with parallel factor analysis, Desalination, 337 (2014) 67-75.
[26] L. Yang, J. Hur, Critical evaluation of spectroscopic indices for organic matter source tracing via end member mixing analysis based on two contrasting sources, Water Res., 59 (2014) 80-89.
[27] Q.V. Ly, T. Maqbool, J. Hur, Unique characteristics of algal dissolved organic matter and their association with membrane fouling behavior: a review, Environmental Science and Pollution Research, (2017) 1-14.
[28] S.A. Huber, A. Balz, M. Abert, W. Pronk, Characterisation of aquatic humic and non-humic matter with size-exclusion chromatography - organic carbon detection - organic nitrogen detection (LC-OCD-OND), Water Res., 45 (2011) 879-885.
[29] T. Maqbool, J. Cho, J. Hur, Spectroscopic descriptors for dynamic changes of soluble microbial products from activated sludge at different biomass growth phases under prolonged starvation, Water Res., 123 (2017) 751-760.
[30] N. Subhi, A.R.D. Verliefde, V. Chen, P. Le-Clech, Assessment of physicochemical interactions in hollow fibre ultrafiltration membrane by contact angle analysis, J. Membr. Sci., 403–404 (2012) 32-40.
[31] W. Huang, H. Chu, B. Dong, J. Liu, Evaluation of different algogenic organic matters on the fouling of microfiltration membranes, Desalination, 344 (2014) 329-338.
[32] T. Lin, Z. Lu, W. Chen, Interaction mechanisms and predictions on membrane fouling in an ultrafiltration system, using the XDLVO approach, J. Membr. Sci., 461 (2014) 49-58.

[33] H. Wang, M. Park, H. Liang, S. Wu, I.J. Lopez, W. Ji, G. Li, S.A. Snyder, Reducing ultrafiltration membrane fouling during potable water reuse using pre-ozonation, Water Res., 125 (2017) 42-51.
[34] B.A. Poulin, J.N. Ryan, G.R. Aiken, Effects of Iron on Optical Properties of Dissolved Organic Matter, Environ. Sci. Technol., 48 (2014) 10098-10106.
[35] F. Qu, H. Liang, J. Zhou, J. Nan, S. Shao, J. Zhang, G. Li, Ultrafiltration membrane fouling caused by extracellular organic matter (EOM) from Microcystis aeruginosa: Effects of membrane pore size and surface hydrophobicity, J. Membr. Sci., 449 (2014) 58-66.
[36] Q.V. Ly, H.-C. Kim, J. Hur, Tracking fluorescent dissolved organic matter in hybrid ultrafiltration systems with TiO2/UV oxidation via EEM-PARAFAC, J. Membr. Sci., (2018).
[37] V.L. Quang, H.-C. Kim, T. Maqbool, J. Hur, Fate and fouling characteristics of fluorescent dissolved organic matter in ultrafiltration of terrestrial humic substances, Chemosphere, 165 (2016) 126-133.
[38] H. Huang, T. Young, J.G. Jacangelo, Novel approach for the analysis of bench-scale, low pressure membrane fouling in water treatment, J. Membr. Sci., 334 (2009) 1-8.
[39] X. Zhang, L. Fan, F.A. Roddick, Effect of feedwater pre-treatment using UV/H2O2 for mitigating the fouling of a ceramic MF membrane caused by soluble algal organic matter, J. Membr. Sci., 493 (2015) 683-689.
[40] D.N. Kothawala, K.R. Murphy, C.A. Stedmon, G.A. Weyhenmeyer, L.J. Tranvik, Inner filter correction of dissolved organic matter fluorescence, Limnol. Oceanogr. Methods, 11 (2013) 616-630.
[41] A.J. Lawaetz, C.A. Stedmon, Fluorescence Intensity Calibration Using the Raman Scatter Peak of Water, Appl. Spectrosc., 63 (2009) 936-940.
[42] C.A. Stedmon, R. Bro, Characterizing dissolved organic matter fluorescence with parallel factor analysis: a tutorial, Limnol. Oceanogr. Methods, 6 (2008) 572-579.
[43] J.A. Brant, A.E. Childress, Assessing short-range membrane–colloid interactions using surface energetics, J. Membr. Sci., 203 (2002) 257-273.
[44] B. Aftab, J. Hur, Fast tracking the molecular weight changes of humic substances in coagulation/flocculation processes via fluorescence EEM-PARAFAC, Chemosphere, 178 (2017) 317-324.
[45] H.-C. Kim, B.A. Dempsey, Membrane fouling due to alginate, SMP, EfOM, humic acid, and NOM, J. Membr. Sci., 428 (2013) 190-197.
[46] S.N. Nam, G. Amy, Differentiation of wastewater effluent organic matter (EfOM) from natural organic matter (NOM) using multiple analytical techniques, Water Sci. Technol., 57 (2008) 1009-1015.
[47] B.-M. Lee, Y.-S. Seo, J. Hur, Investigation of adsorptive fractionation of humic acid on graphene oxide using fluorescence EEM-PARAFAC, Water Res., 73 (2015) 242-251.
[48] D.D. Phong, J. Hur, Insight into photocatalytic degradation of dissolved organic matter in UVA/TiO2 systems revealed by fluorescence EEM-PARAFAC, Water Res., 87 (2015) 119-126.
[49] B.-M. Lee, J. Hur, Adsorption Behavior of Extracellular Polymeric Substances on Graphene Materials Explored by Fluorescence Spectroscopy and Two-Dimensional Fourier Transform Infrared Correlation Spectroscopy, Environ. Sci. Technol., 50 (2016) 7364-7372.
[50] J.B. Fellman, E. Hood, R.G.M. Spencer, Fluorescence spectroscopy opens new windows into dissolved organic matter dynamics in freshwater ecosystems: A review, Limnol. Oceanogr., 55 (2010) 2452-2462.

634 [51] E.L. Sharp, P. Jarvis, S.A. Parsons, B. Jefferson, Impact of fractional character on the
635 coagulation of NOM, Colloids Surf. Physicochem. Eng. Aspects, 286 (2006) 104-111.
636 [52] Z. Yuan, C. He, Q. Shi, C. Xu, Z. Li, C. Wang, H. Zhao, J. Ni, Molecular Insights into the
637 Transformation of Dissolved Organic Matter in Landfill Leachate Concentrate during
638 Biodegradation and Coagulation Processes Using ESI FT-ICR MS, Environ. Sci. Technol., 51
639 (2017) 8110-8118.
640 [53] C. Jarusutthirak, G. Amy, Understanding soluble microbial products (SMP) as a component
641 of effluent organic matter (EfOM), Water Res., 41 (2007) 2787-2793.
642 [54] V.L. Quang, I. Choi, J. Hur, Tracking the behavior of different size fractions of dissolved
643 organic matter in a full-scale advanced drinking water treatment plant, Environ. Sci. Pollut. Res.,
644 22 (2015) 18176-18184.
645 [55] R.K. Henderson, S.A. Parsons, B. Jefferson, The impact of differing cell and algogenic
646 organic matter (AOM) characteristics on the coagulation and flotation of algae, Water Res., 44
647 (2010) 3617-3624.
648 [56] C. Ayache, M. Pidou, J.P. Croué, J. Labanowski, Y. Poussade, A. Tazi-Pain, J. Keller, W.
649 Gernjak, Impact of effluent organic matter on low-pressure membrane fouling in tertiary
650 treatment, Water Res., 47 (2013) 2633-2642.
651 [57] Z. Yan, B. Liu, F. Qu, A. Ding, H. Liang, Y. Zhao, G. Li, Control of ultrafiltration
652 membrane fouling caused by algal extracellular organic matter (EOM) using enhanced Al
653 coagulation with permanganate, Sep. Purif. Technol., 172 (2017) 51-58.
654 [58] D.T. Myat, M.B. Stewart, M. Mergen, O. Zhao, J.D. Orbell, S. Gray, Experimental and
655 computational investigations of the interactions between model organic compounds and
656 subsequent membrane fouling, Water Res., 48 (2014) 108-118.
657 [59] F. Xiao, P. Xiao, W.J. Zhang, D.S. Wang, Identification of key factors affecting the organic
658 fouling on low-pressure ultrafiltration membranes, J. Membr. Sci., 447 (2013) 144-152.
659 [60] L. De Angelis, M.M.F. de Cortalezzi, Ceramic membrane filtration of organic compounds:
660 Effect of concentration, pH, and mixtures interactions on fouling, Sep. Purif. Technol., 118
661 (2013) 762-775.
662 [61] C.-W. Jung, H.-J. Son, L.-S. Kang, Effects of membrane material and pretreatment
663 coagulation on membrane fouling: fouling mechanism and NOM removal, Desalination, 197
664 (2006) 154-164.
665 [62] M. Zhou, F. Meng, Aluminum-induced changes in properties and fouling propensity of
666 DOM solutions revealed by UV–vis absorbance spectral parameters, Water Res., 93 (2016) 153-
667 162.
668 [63] M. Zhou, F. Meng, Using UV–vis absorbance spectral parameters to characterize the
669 fouling propensity of humic substances during ultrafiltration, Water Res., 87 (2015) 311-319.
670 [64] C.-F. Lin, A. Yu-Chen Lin, P. Sri Chandana, C.-Y. Tsai, Effects of mass retention of
671 dissolved organic matter and membrane pore size on membrane fouling and flux decline, Water
672 Res., 43 (2009) 389-394.
673 [65] L.O. Villacorte, Y. Ekowati, H. Winters, G. Amy, J.C. Schippers, M.D. Kennedy, MF/UF
674 rejection and fouling potential of algal organic matter from bloom-forming marine and
675 freshwater algae, Desalination, 367 (2015) 1-10.
676 [66] A.W. Zularisam, A.F. Ismail, R. Salim, Behaviours of natural organic matter in membrane
677 filtration for surface water treatment — a review, Desalination, 194 (2006) 211-231.

[67] X. Zhang, L. Fan, F.A. Roddick, Understanding the fouling of a ceramic microfiltration membrane caused by algal organic matter released from Microcystis aeruginosa, J. Membr. Sci., 447 (2013) 362-368.
[68] A.S. Al-Amoudi, Factors affecting natural organic matter (NOM) and scaling fouling in NF membranes: A review, Desalination, 259 (2010) 1-10.

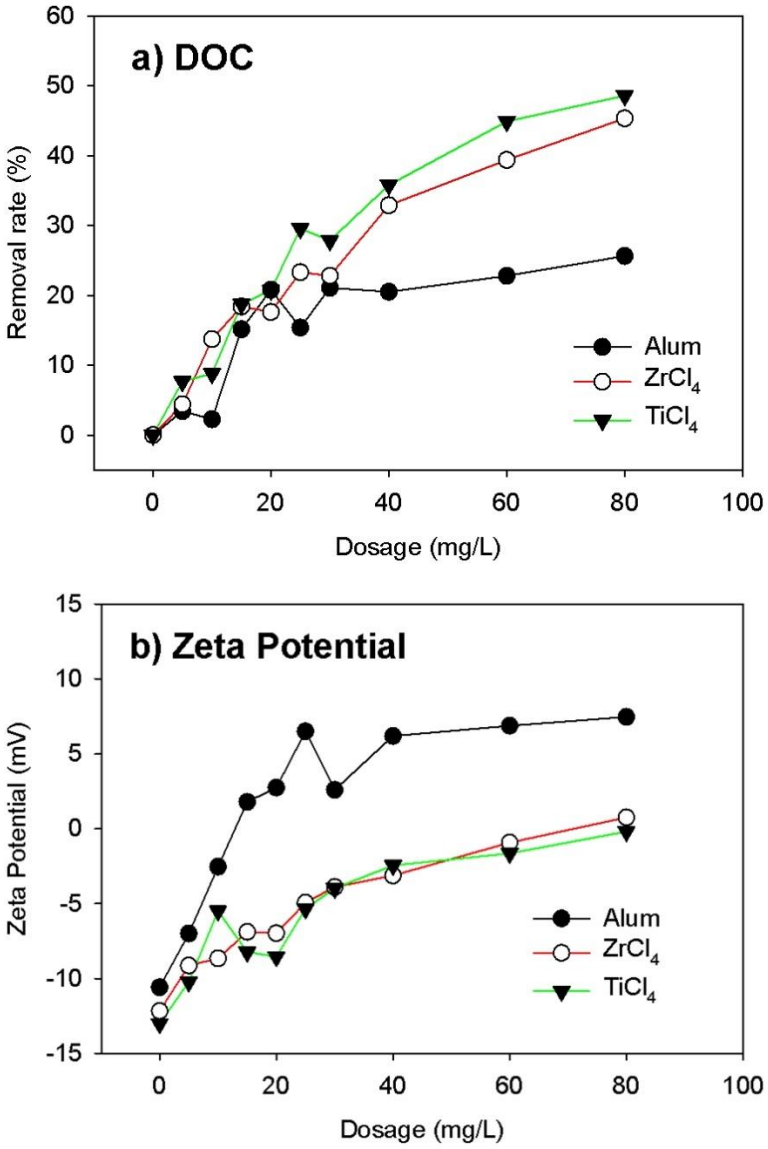

687

688

689 Fig. 1. (a) EfOM removal by coagulation measured as DOC and (b) zeta potential of the flocs particles
690 when using $Al_2(SO_4)_3$, $ZrCl_4$ and $TiCl_4$ coagulant.

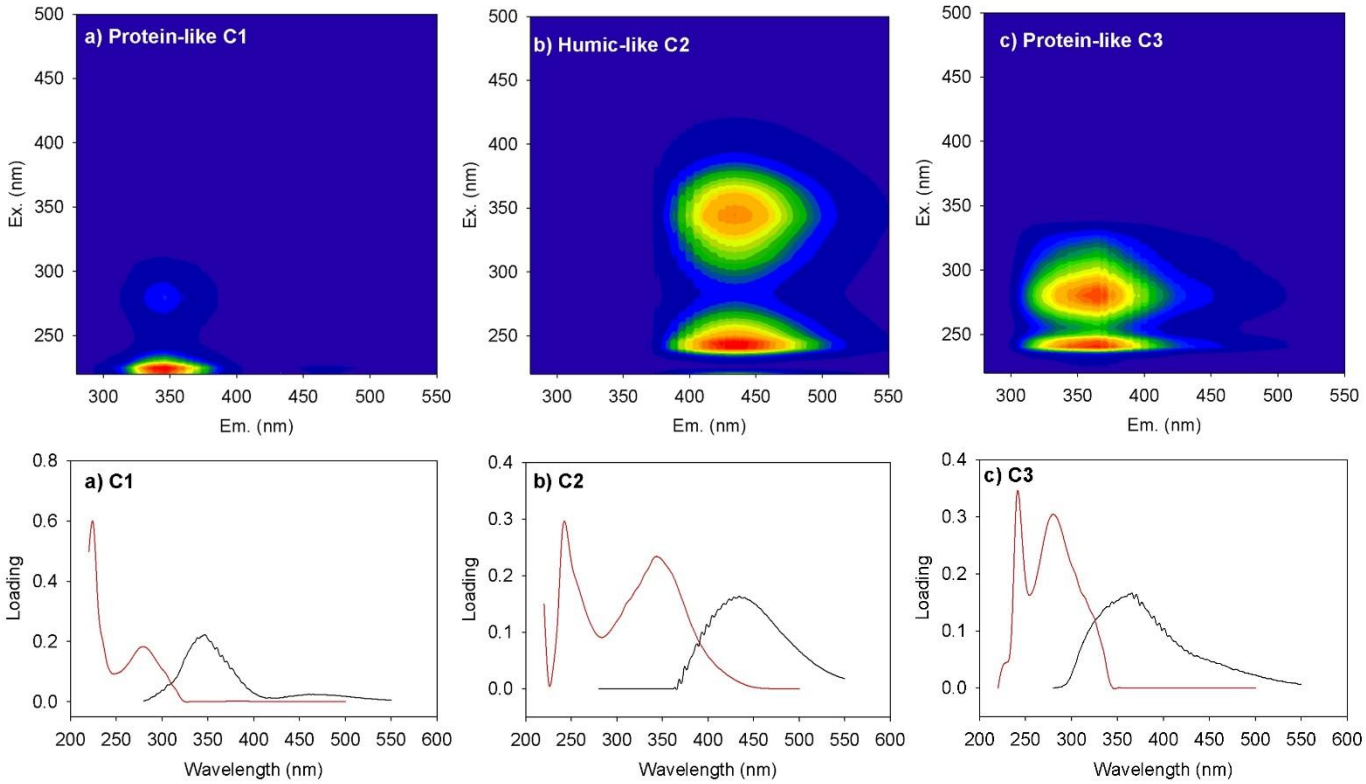

Fig. 2. Three individual fluorescent components (protein-like C1, humic-like C2, and protein-like C3) (above) identified by EEM-PARAFAC modelling, and the corresponding Ex/Em loadings validated by split half analysis (below).

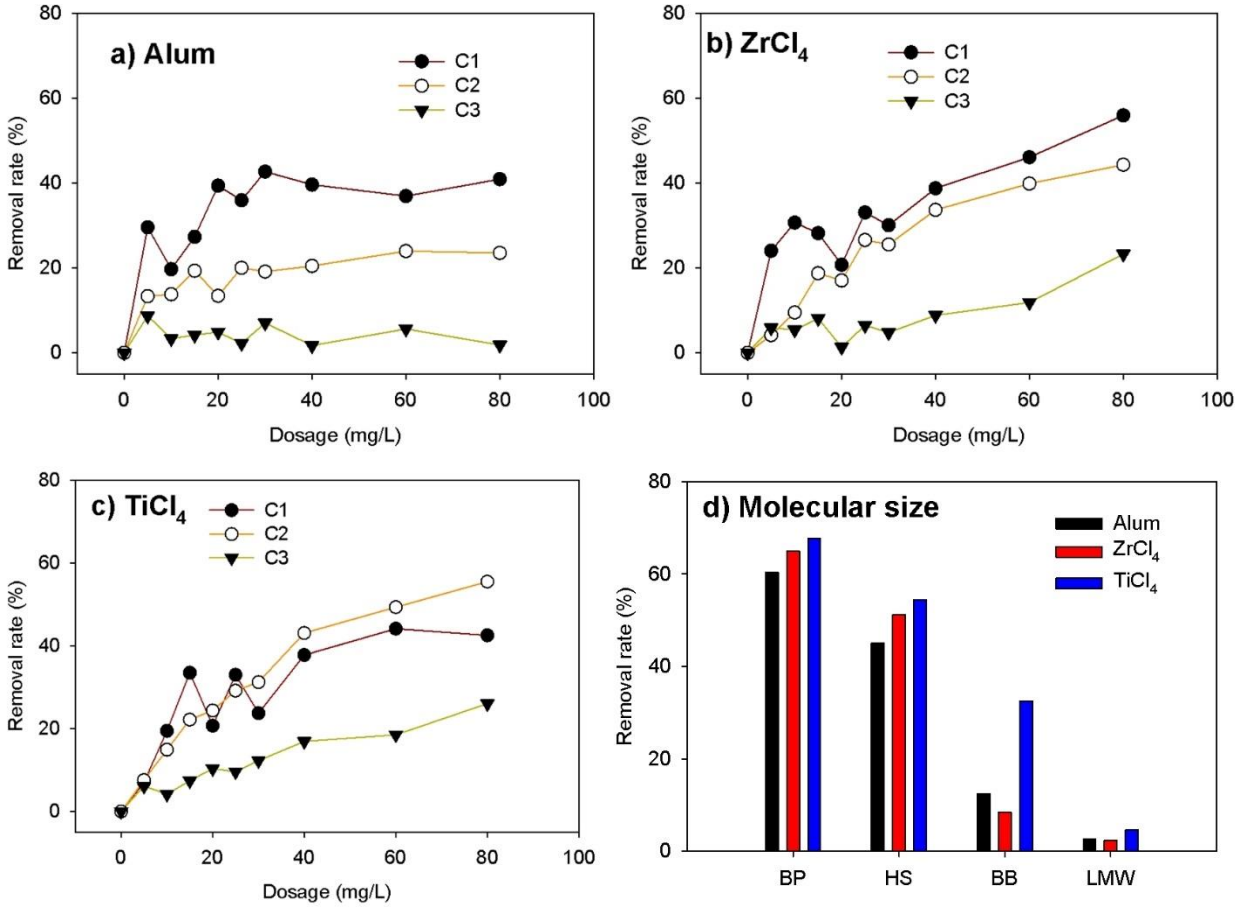

Fig. 3. The rate of removal of different FDOM components by (a)Alum, (b)$ZrCl_4$, and (c) $TiCl_4$ measured by EEM-PARAFAC. The removal rates of different size fractions, determined by SEC-OCD, at the optimum dosage of each coagulant (d).

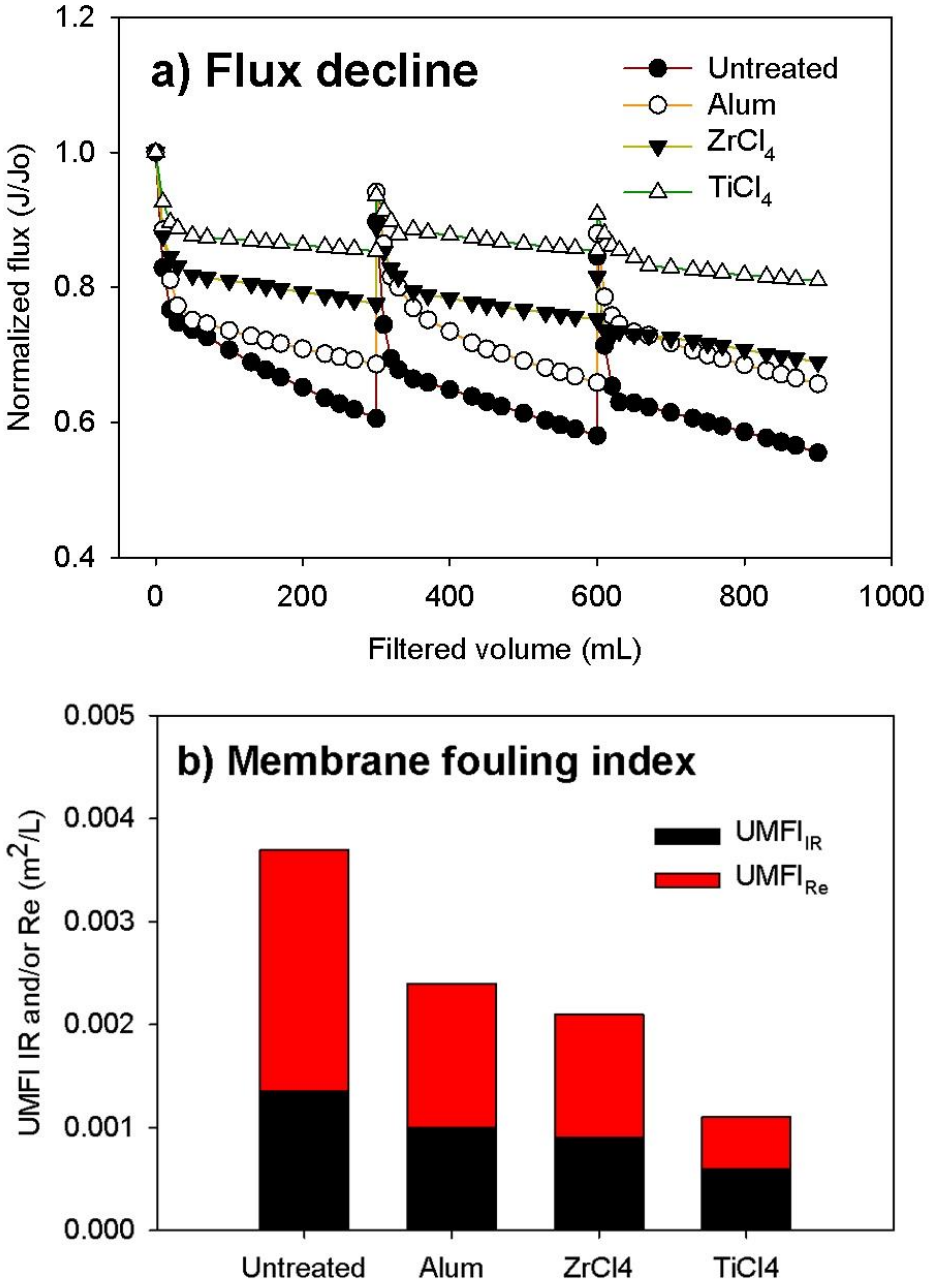

11

12

13 Fig. 4. Flux profile of a) of untreated (or original) EfOM, and treated EfOM with $Al_2(SO_4)_3$, $ZrCl_4$, and
14 $TiCl_4$ and their corresponding membrane fouling index $UMFI_{Re}$ and $UMFI_{IR}$. The sum of the reversible and
15 the irreversible fouling index is equivalent to the total fouling index (i.e., $UMFI_{Total}$).

16

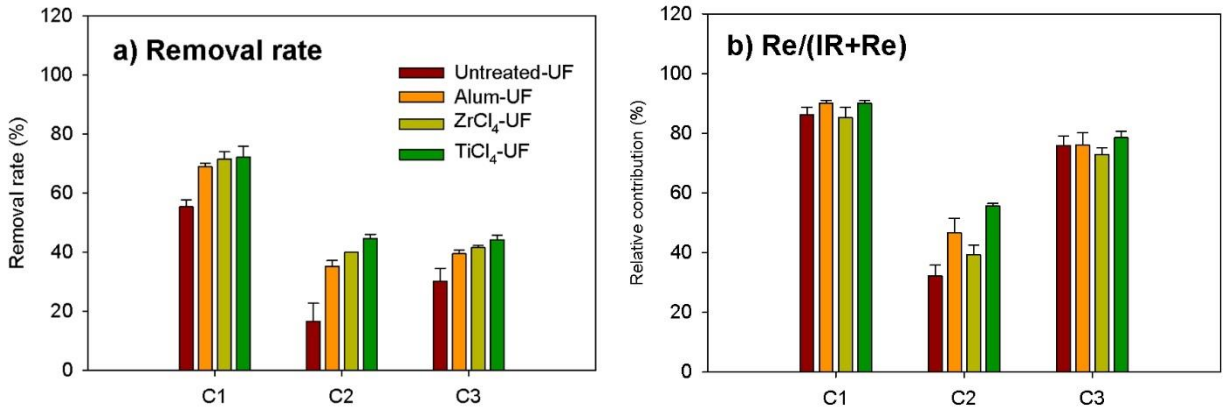

Fig. 5. Comparison of the behaviors of individual FDOM components in the untreated and the treated EfOM with respect to a) the removal rate and b) the relative contributions to reversible membrane fouling potential. Error bars are based on duplicate experiments.

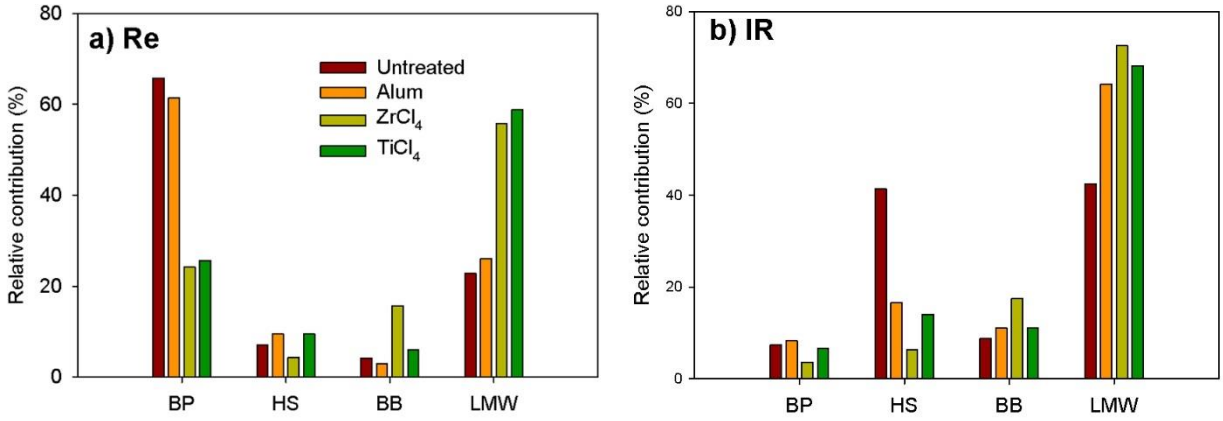

Fig. 6. Relative contributions of different size fractions in the untreated and the treated EfOM to a) reversible fouling and b) irreversible fouling.

Table 1. Regression coefficient (R^2) for untreated and treated EfOM by different coagulations upon four classical fouling mechanisms

	Untreated	**Alum**	**$ZrCl_4$**	**$TiCl_4$**
Complete Blocking	0.832	0.771	0.695	0.713
Standard Blocking	0.994	0.996	0.994	0.997
Intermediate Blocking	0.821	0.732	0.756	0.672
Cake/gel layer	0.952	0.792	0.878	0.752

Table 2. Surface tension parameters, interfacial free energy of cohesion (ΔG_{iLi}^{TOT}) and adhesion (ΔG_{iLm}^{TOT}) after virgin membrane, untreated and treated EfOM upon the C/F processes.

	δ^{LW}	δ^{+}	δ^{-}	δ^{AB}	δ^{TOT}	ΔG_{iLi}^{TOT}	ΔG_{iLm}^{LW}	ΔG_{iLm}^{AB}	ΔG_{iLm}^{TOT}
PES membrane	49.19	0.55	22.54	7.05	56.24	-16.20			
Untreated	50.29	0.44	11.65	4.55	54.84	-40.42	-11.36	-16.74	-28.10
Alum-treated	43.24	0.01	21.85	1.05	44.29	-14.68	-8.94	-6.21	-15.16
$ZrCl_4$-treated	41.39	0.33	28.31	6.14	47.52	-1.38	-8.27	-0.37	-8.64
$TiCl_4$-treated	41.55	0.12	30.88	3.83	45.38	3.23	-8.33	1.52	-6.81

Nomenclature

LW	:	Lifshitz – Van der Waals interactions
AB	:	short-range acid-base interactions
EL	:	electrostatic double layer interactions
δ^+	:	electron-accepting component (mJ/m^2)
δ^-	:	electron-donating component (mJ/m^2)
δ^{LW}	:	Lifshitz – Van der Waals component of surface free energy (mJ/m^2)
δ^{AB}	:	acid-base component of surface free energy (mJ/m^2)
δ^{EL}	:	electrostatic double layer component of surface free energy (mJ/m^2)
L	:	probe liquid(s) (i.e. DDW, Diiodomethane, Glycerin)
m	:	virgin membrane surface
i	:	solid surface i.e. virgin or foulants
θ	:	contact angle (degree)
ΔG_{iLi}^{LW}	:	LW component of cohesion free energy (mJ/m^2)
ΔG_{iLi}^{AB}	:	AB component of cohesion free energy (mJ/m^2)
ΔG_{iLi}^{TOT}	:	total interfacial free energy of cohesion (mJ/m^2)
ΔG_{iLm}^{LW}	:	LW component of adhesion free energy (mJ/m^2)
ΔG_{iLm}^{AB}	:	AB component of adhesion free energy (mJ/m^2)
ΔG_{iLm}^{TOT}	:	total interfacial free energy of adhesion (mJ/m^2)